

Synthesis and characterizations of $\text{Cu}_2\text{MgSnS}_4$ nanoparticles by solvothermal method

H. Guan*, J. X. Xu, Z. Y. Yang, X. Y. Qian, M. Q. Zhao
*School of Materials Science and Engineering, Yancheng Institute of Technology, 9
Yinbing Street, Yancheng 224051, PR China*

$\text{Cu}_2\text{MgSnS}_4$ (CMTS) nanoparticles are successfully prepared via a solvothermal approach. X-ray diffraction (XRD) and Raman reveal that pure zinc-blende CMTS phase is obtained. Scanning electron microscopy (SEM) shows that CMTS nanoparticles exhibit microsphere structure. The band gap of as-obtained CMTS nanoparticles is calculated to be 1.68eV, indicating a potential candidate for tandem solar cells. The degradation rate of methylene blue (MB) with under visible-light irradiation is about 87%, indicating that CMTS can be useful for effective visible-light photocatalyst.

(Received November 12, 2023; Accepted February 12, 2024)

Keywords: Semiconductors, $\text{Cu}_2\text{MgSnS}_4$, Nanocrystals, Solvothermal, Optical, Photocatalytic

1. Introduction

In decades, chalcogenide semiconductor materials, such as CuInSe_2 , $\text{Cu}_2\text{InGa}(\text{Se,S})_4$, CdTe , Bi_2Te_3 , PbTe , etc., have attracted wide attention and in-depth study for applications in the fields of photovoltaic, photocatalysis and thermoelectric[1-5]. Recently, many studies have been performed on the development of earth-abundant, cheaper and environment friendly chalcogenide materials due to the limitation of the rarity of indium(In) and tellurium(Te) and the toxicity of cadmium(Cd). As a result of the studies above, $\text{Cu}_2\text{ZnSnS}_4$ (CZTS) exhibits high absorption coefficients($>10^4\text{cm}^{-1}$), band gap in the optimal light absorption range (1.0~1.5eV) and all constituents are abundant in the crust of the earth [6-10]. $\text{Cu}_2\text{MgSnS}_4$ (CMTS) is also considered as a good alternative material for energy applications due to its similar structure as CZTS. Over the past few years, quaternary compound CMTS have been synthesized by some methods such as ultrasonic co-spray pyrolysis, hot-injection, sol-gel, co-precipitation, and pulsed laser deposition, and the CMTS structure was further studied by first-principles [11-17]. However, no reports have been found to synthesis CMTS nanoparticles via solvothermal method.

In this paper, we report the solvothermal method to synthesis CMTS nanoparticles, and investigate their structure, morphology, optical and photocatalytic properties.

2. Experimental details

Copper chloride dihydrate ($\text{CuCl}_2\cdot 2\text{H}_2\text{O}$, 99%), Magnesium chloride hexahydrate ($\text{MgCl}_2\cdot 6\text{H}_2\text{O}$, 98%), Tin(II) chloride dihydrate ($\text{SnCl}_2\cdot 2\text{H}_2\text{O}$, 98%), Cadmium chloride hemi ($\text{CdCl}_2\cdot 2.5\text{H}_2\text{O}$, 99%) and Thiourea (H_2NCSNH_2 , 99%) are supplied from Sinopharm Chemical Reagent Co. Ltd. In a typical procedure, $\text{CuCl}_2\cdot 2\text{H}_2\text{O}$ (0.002M), $\text{MgCl}_2\cdot 6\text{H}_2\text{O}$ (0.001M), $\text{SnCl}_2\cdot 2\text{H}_2\text{O}$ (0.001M) and H_2NCSNH_2 (0.006M) are dissolved in 80ml ethylene glycol (EG) as precursor. The precursor solutions are stirred for 2h, then transferred into autoclaves and maintained at 200°C for 12h. The autoclaves are naturally cooled down to room temperature. At last, the products are washed several times with deionized water and dried in vacuum at 80°C for 3h for further use.

* Corresponding author: guan hao1980@sina.com
<https://doi.org/10.15251/CL.2024.212.169>

The crystal phase is measured by X-ray diffraction (PaNalytical X'Pert Pro) and Raman spectroscopy (JY-T64000). The morphology is investigated by scanning electron microscope (LEO-1530VP). The optical property is measured by spectrophotometer (Shimadzu UV-2450). The photocatalytic property is measured by Shimadzu UV2450 spectrophotometer.

3. Results and discussion

The XRD result of the synthesized CMTS nanoparticles is depicted in Fig.1(a). It can be seen that the major diffraction peaks at $2\theta=28.68^\circ$, 32.7° , 47.52° and 56.24° are in agreement with the respective (111), (200), (220) and (311) planes of zinc-blende structure with a space group of F-43m(JCPDS no. 216). The lattice parameters calculated from the XRD pattern are $a=b=c=5.39\text{\AA}$. No other characteristic peaks from other crystalline forms are noticed, indicating that no secondary phases are present. The plane also shows the broad full-width at half-maxima, indicating the formation of nano crystallinity. According to the Debye-Scherrer formula, the average crystallite size of CMTS can be calculated as 23.6nm.

Raman spectrum of the synthesized CMTS nanoparticles is recorded to further confirm the structure owing to the similarity of the XRD patterns of zinc-blende CMTS and Cu_2SnS_3 (JCPDS no.27-0198). As shown in Fig.1(b), it can be observed that the domain peaks at 333cm^{-1} . Also, the absence of Raman peaks corresponding to Cu_2SnS_3 (267cm^{-1} , 303cm^{-1} and 352cm^{-1}) exclude the presence, indicating the single phase of CMTS nanocrystals, which is in accordance with the XRD result.

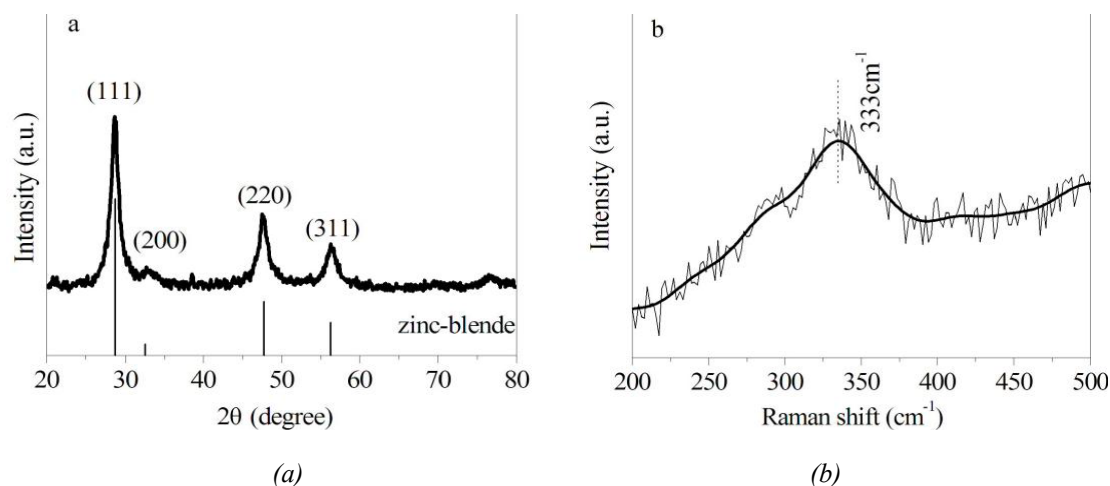


Fig. 1. XRD pattern(a) and Raman spectrum(b) of CMTS nanoparticles.

The general morphology of the synthesized CMTS nanoparticles is presented in Fig.2. It indicates that CMTS microspheres with approximately 1-2 μm in diameter are formed. As shown in inset image, which are formed by agglomeration of small nanocrystals with the grain sizes of about 20nm corresponding to the results obtained by XRD analysis.

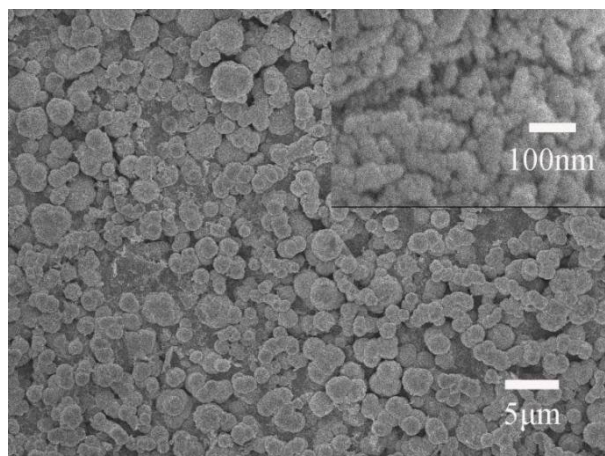


Fig. 2. Low magnification SEM images of CMTS nanoparticles; Inset: high magnification SEM images of CMTS nanoparticles.

The optical band gap energy of the synthesized CMTS nanoparticles is determined by plotting $(\alpha hv)^2$ against hv . The band gap of zinc-blende CMTS phase is determined to be 1.68 eV, as shown in Fig.3, implying that the calculated band-gap value is compatible with the result in the literature [12], which is suitable for energy application.

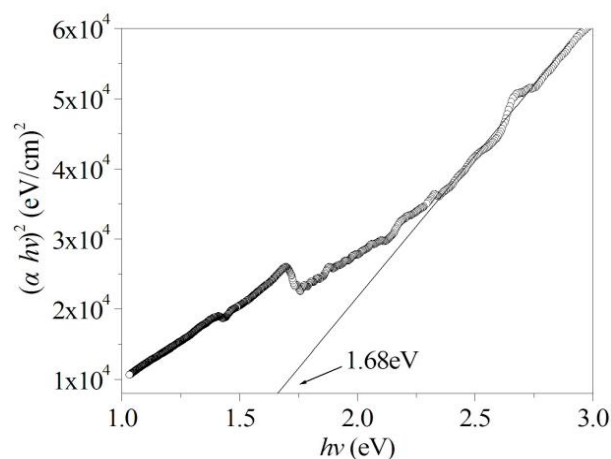


Fig. 3. Optical bandgap estimation of CMTS nanoparticles.

In order to evaluate of the photocatalytic property of CMTS nanoparticles, we examine the decomposition of methylene blue (MB) under visible-light irradiation for different time, in which MB is chosen as a typical organic waste model. The photocatalytic degradation rates (C/C_0) of the MB with and without CMTS nanoparticles are shown in Fig.4. It can be seen that MB without CMTS decomposes only about 2%, indicating that self-degradation of MB could be neglected. While that with the addition of CMTS decreases almost at 87% after 100min illumination. The results demonstrate that CMTS is an excellent applicant of visible-light photocatalyst.

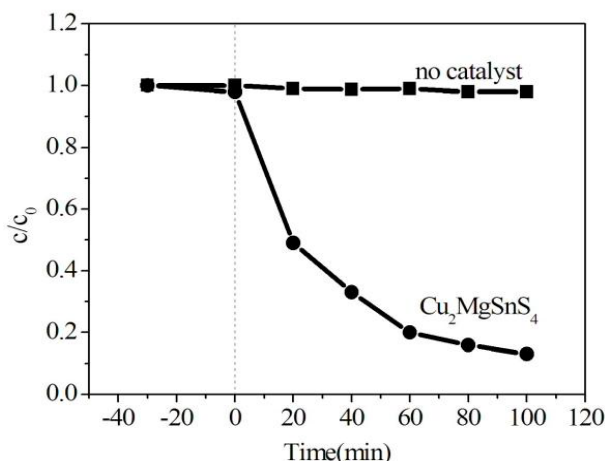


Fig. 4. The photodegradation rate of MB as a function of different time with and without the addition of CMTS nanoparticles.

4. Conclusions

In the present work, pure CMTS nanoparticles are firstly synthesized via the solvothermal method. The prepared CMTS exhibits microsphere structure. The optical bandgap of the CMTS nanoparticles is around 1.68eV, indicating suitable optical properties for tandem solar cell applications. The synthesized CMTS nanoparticles could degrade about 87% of the methylene blue (MB) within 100min under visible-light irradiation, indicating a potential candidate for visible-light photocatalyst to treating pollutants in waste water.

References

- [1] M. Bär, I. Repins, M. A. Contreras, L. Weinhardt, R. Noufi, C. Heske, *Appl. Phys. Lett.* **95**, 052106 (2009); <https://doi.org/10.1063/1.3194153>
- [2] M. Bagheri, A. R. Mahjoub, B. Mehri, *RSC Adv.* **4**, 21757; (2014). <https://doi.org/10.1039/c4ra01753f>
- [3] V. A. Akhavan, M. G. Panthani, B. W. Goodfellow, D. K. Reid, B. A. Korgel, *Opt. Express* **18**, A411 (2010); <http://doi.org/10.1364/OE.18.00A411>
- [4] M. G. Kanatzidis, *Chem. Mater.* **22**, 648 (2010); <http://doi.org/10.1021/cm902195j>
- [5] Q. Guo, G. M. Ford, H. W. Hillhouse, R. Agrawal, *Nano. Lett.* **9**, 3060 (2009); <http://doi.org/10.1021/nl901538w>
- [6] Z. Zhou, Y. Wang, D. Xu, Y. Zhang, *Sol. Energy Mater. Sol. Cells* **94**, 2042 (2010); <http://doi.org/10.1016/j.solmat.2010.06.010>
- [7] J. Huang, C. Yan, K. Sun, F. Liu, H. Sun, A. Pu, X. Liu, M. Green, X. Hao, *Sol. Energy Mater. Sol. Cells* **175**, 71 (2018); <http://doi.org/10.1016/j.solmat.2017.10.009>
- [8] R. Chong, X. Wang, Z. Chang, W. Zhou, S. Wu, *Int. J. Hydrogen Energy* **42**, 20703 (2017); <http://doi.org/10.1016/Ahydene.2017.06.231>
- [9] M. Z. Ansari, M. Faraz, S. Munjal, V. Kumar, N. Khare, *Adv. Powder Tech.* **28**, 2402 (2017); <https://doi.org/10.1016/j.appt.2017.06.023>
- [10] M. Zubair, A. Razzaq, C. A. Grimes, S. In, *J CO₂ Util.* **20**, 301 (2017); <http://doi.org/10.1016/j.jcou.2017.05.021>
- [11] Y. Guo, W. Cheng, J. Jiang, S. Zuo, F. Shi, J. Chu, *Mater. Lett.* **172**, 68 (2016). <http://doi.org/10.1016/j.matlet.2016.02.088>
- [12] M. Wei, Q. Du, R. Wang, G. Jiang, W. Liu, C. Zhu, *Chem. Lett.* **43**, 1149 (2014); <http://doi.org/10.1246/cl.140208>
- [13] G. Yang, X. Zhai, Y. Li, B. Yao, Z. Ding, R. Deng, H. Zhao, L. Zhang, Z. Zhang, *Mater. Lett.* **242**, 58 (2019); <https://doi.org/10.1016/j.matlet.2019.01.102>

- [14] A. Sharma, P. Sahoo, A. Singha, S. Padhan, G. Udayabhanu, R. Thangavel, Sol. Energy **203**, 284 (2020); <https://doi.org/10.1016/j.solener.2020.04.027>
- [15] A. Ali, Y. Liang, S. Ahmed, B. Yang, B. Guo, Y. Yang, Appl. Mater. Today **18**, 100534 (2020); <https://doi.org/10.1016/j.apmt.2019.100534>
- [16] G. L. Agawane, S. A. Vanalakar, A. S. Kamble, A. V. Moholkar, J. H. Kimf, Mater. Sci. Semicond. Process. **76**, 50 (2018); <https://doi.org/10.1016/j.mssp.2017.12.010>
- [17] S. Sharma, P. Kumar, J. Phys. Commun. **1**, 045014 (2017); <http://doi.10.1088/2399-6528/aa9286>